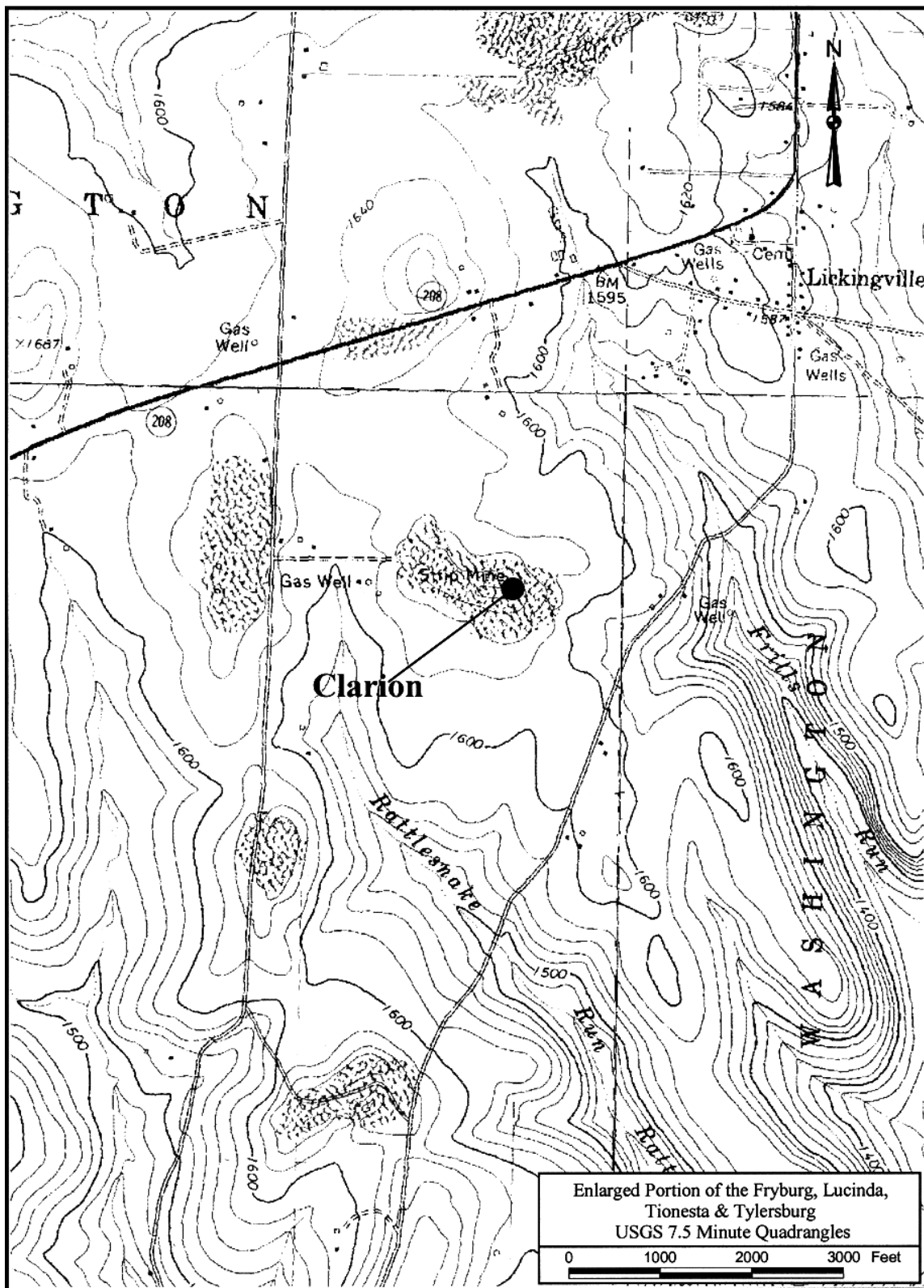


Chapter 5: Analysis of Data from the Clarion Site

The Clarion mine site is located in northern Clarion County, Pennsylvania, in the northwestern portion of the bituminous coal region. The acid mine discharge (S3CLAR) was from an abandoned surface mine on the Upper and Lower Clarion coal seams that was the site of abandoned mine reclamation and a cooperative research project by the Bureau of Abandoned Mine Reclamation of the Pennsylvania Department of Environmental Resources and the U.S. Bureau of Mines. During this project, alkaline addition (in the form of crushed limestone) was incorporated into the reclamation procedures as an attempt to reduce the acid mine drainage pollution, as described by Lusardi and Erickson (1985). A map of the Clarion site is shown in Figure 5.1, which is adapted from Lusardi and Erickson (1985).

The data set used for most of the statistical analysis of the Clarion site contains 96 samples for the time period from December 15, 1981 to August 4, 1986. Of these data, approximately half ($N = 49$) are pre-treatment, and the other half ($N = 47$) are post-treatment with the crushed limestone, alkaline-addition reclamation procedure. Missing data presented a problem in the statistical analysis of the discharge and water quality characteristics.

Figure 5.1: Map of Clarion Mine Site



Univariate Analysis

Initially, there were 104 observations in this data set. However, at least 19 samples were missing flow measurements, and others were missing one or more water quality parameters. Discharge and pH were plotted against date to see where the largest gaps occurred. After careful examination, the data set was reduced to 96 rows containing seven columns: pH, discharge, acidity, total iron, sulfate, ferrous iron, and ferric iron. Ferric iron is determined by subtracting ferrous iron from total iron. The statistics describing the variables were derived and mean values were inserted in rows with missing values. The data were then rerun to yield Table 5.1.

Table 5.1: Summary Statistics for S3CLAR (N=96)

	N	N*	Mean	Median	Trimmed Mean	Standard Deviation	Standard Error of the Mean
pH	96	0	3.696	3.195	3.612	0.985	0.101
Discharge	79	17	12.57	6.70	9.09	22.37	2.52
Acidity	96	0	522.4	483.5	505.6	346.4	35.4
Total Iron	96	0	82.40	75.00	79.31	51.01	5.21
Ferrous Iron	96	0	48.38	37.75	45.97	34.46	3.52
SO ₄	96	0	1528.4	1569.0	1525.9	566.0	57.8
Ferric Iron	96	0	34.02	23.60	31.44	32.05	3.3

	Minimum	Maximum	First Quartile	Third Quartile	Coefficient of Variation
pH	2.670	6.430	3.002	4.455	26.6
Discharge	0.05	172.00	3.60	12.48	178.0
Acidity	1.0	1546.0	232.5	737.7	66.3
Total Iron	8.70	257.00	39.70	110.25	61.9
Ferrous Iron	0.90	143.00	23.87	66.65	71.2
SO ₄	296.0	3241.0	1181.5	1878.2	37.0
Ferric Iron	- 4	152.00	6.00	55.00	94.2

The very high magnitude of variation in discharge is shown by the value of the Coefficient of Variation ($CV\% = \text{standard deviation}/\text{mean} * 100$) = 180.1%. The coefficients of variation for pH and sulfate are reasonable. However, the CV% for acidity and all iron parameters are rather large. Correction for some exceptional values is proposed when the variables take values which are either very unlikely or even sometimes impossible.

The frequency distribution for sulfate appears to be symmetrical (Figure 5.2). However, some variables exhibit positive skewness including discharge (Figure 5.3a) and acidity (Figure 5.4a). Attempts were made to make these frequency distributions more symmetrical by transforming to logarithms, but this transformation over-corrected and resulted in negative skewness.

For example, log discharge (Figure 5.3b) is slightly negatively skewed and log acidity is extremely skewed (Figure 5.4b). It was decided, therefore, to use the data without transformation.

Figure 5.2: Stem-and-leaf of Sulfate

```
N = 96
Leaf Unit = 100
4      0      2333
6      0      45
10     0      677
17     0      8889999
26     1      000011111
38     1      222223333333
(12)   1      444445555555
46     1      6666666667777777
29     1      8888889999
19     2      000011111
10     2      22223
5      2      44
3      2      6
2      2      8
1      3
1      3      2
```

Figure 5.3a: Stem-and-leaf of Discharge

N = 77
 Leaf Unit = 1.0 N* = 19

(53)	0	0000000000111122233333334444455555555666667788999999
24	1	00222244444
13	2	001288
7	3	066
4	4	0
3	5	0
2	6	
2	7	
2	8	3
1	9	
1	10	
1	11	
1	12	
1	13	
1	14	
1	15	
1	16	
1	17	2

Figure 5.3b: Stem-and-Leaf of Log Discharge

N = 75
 Leaf Unit = 0.10 N* = 22

4	-1	3000
7	-0	766
11	-0	4330
19	0	01124444
(35)	0	55555666667777777778888899999999
21	1	000111111333344
6	1	55679
1	2	2

Due to the 19 missing discharge values, a second modified data set was prepared by omitting each row with a missing value for discharge; this left 79 rows with complete observations. This step was essential to the study of the association between discharge and other parameters using plotting routines or cross-correlation. Summary statistics for the modified data set are presented in Table 5.2.

Table 5.2: Summary Statistics for S3CLAR Adjusted Data Deck (N=79)

	N	Mean	Median	Trimmed mean	Standard Deviation	Standard Error of the Mean
pH	79	3.624	3.160	3.533	0.967	0.109
Discharge	79	12.57	6.70	9.09	22.37	2.52
Acidity	79	556.1	499.0	542.1	361.2	40.6
Total Iron	79	86.70	78.50	83.80	53.45	6.01
Ferrous Iron	79	51.23	40.00	49.01	35.92	4.04
SO ₄	79	1586.3	1619.0	1578.6	559.6	63.0
Ferric Iron	79	35.47	26.00	32.89	33.80	3.80

	Minimum	Maximum	First Quartile	Third Quartile	Coefficient of Variation
pH	2.670	6.430	2.950	4.050	26.7
Discharge	0.05	172.00	3.60	12.48	178.0
Acidity	1.0	1546.0	234.0	819.0	65.0
Total Iron	8.70	257.00	43.00	118.00	61.6
Ferrous Iron	0.90	143.00	25.50	73.50	70.1
SO ₄	364.0	3241.0	1193.0	1948.0	35.3
Ferric Iron	-4.00	152.00	6.00	55.20	95.3

In this adjusted data set (N=79), the coefficients of variation for pH, discharge, acidity, total iron, and sulfate remain close to the same values even after adjustment. CV% for ferrous iron and ferric iron were greatly reduced. The frequency distributions showed similar positive skewness except for sulfate which appeared essentially symmetrical.

Bivariate Analysis

In order to have a measure of the degree of linear association among pairs of variables and to ensure that any relationship is not obscured by time lags, cross-correlation functions for each parameter were obtained (Figure 5.5 for N=79 observations). Discharge and pH showed their maximum degree of association at zero lag (0.357, Figure 5.5a) and it is suspected that the value of this relationship is inflated by the one exceptional value. In other words, it is doubtful that these data could be used to substantiate any real degree of association. The maximum degree of association between acidity and discharge is -0.3 (Figure 5.5b); the direction of association (increase of acidity with decrease of discharge) is likely to be correct, but the degree ($r^2 = 9\%$) is

very small. Similarly, sulfate and discharge show several values of cross-correlation greater than 0.2 at lags of 0, 7, 8, and -15, so that no real association can be claimed (Figure 5.5c).

The use of the cross-correlation function in bivariate and time series analyses is discussed in Chapters 3 through 9 of this report. In these chapters, an r value of 0.2 or a more conservative value of 0.3 have been arbitrarily selected as critical values, with the inference that r values of less than these critical values are not significantly different than 0, and therefore can be deleted from consideration. These arbitrary critical values were selected by rounding off the values of r that are significant at the 5% level for the sample sizes contained in this report (e.g., for this data set of the Clarion discharge where $N = 96$, the value of r that is significant at the 5% level with 90 degrees of freedom is 0.205 (Table 22 in Arkin and Colton, 1963, p.155)).

Figure 5.5a: Cross Correlation Function for pH and Discharge

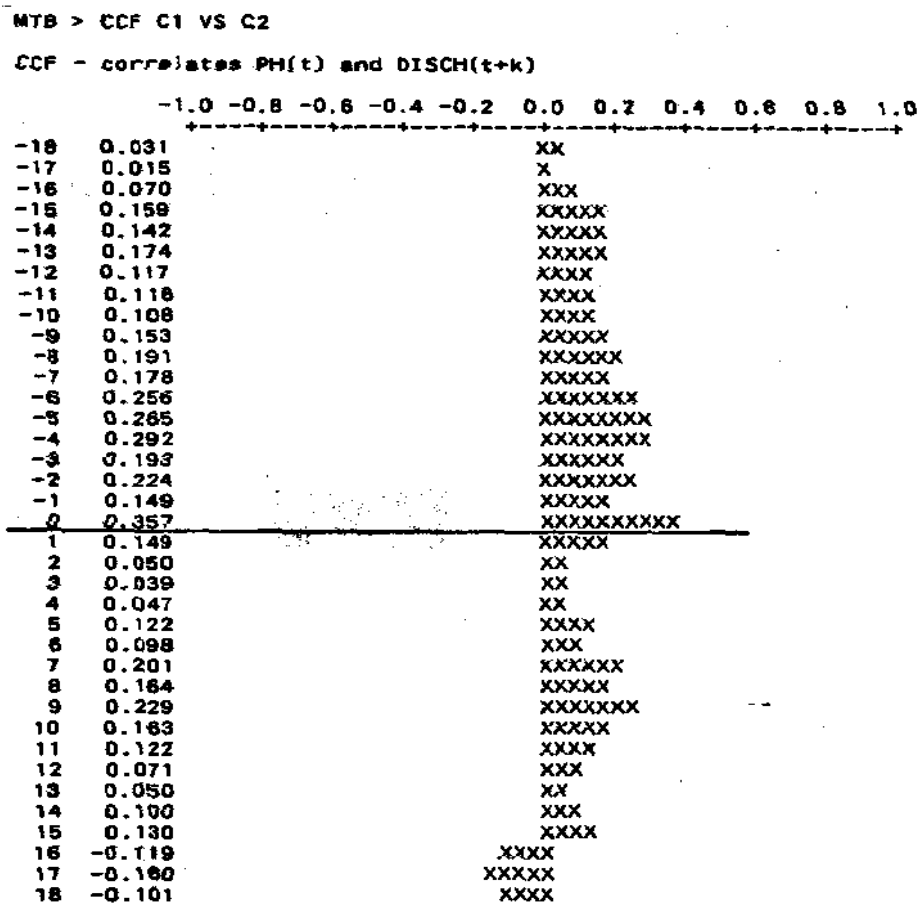


Figure 5.5b: Cross Correlation Function for Acidity and Discharge

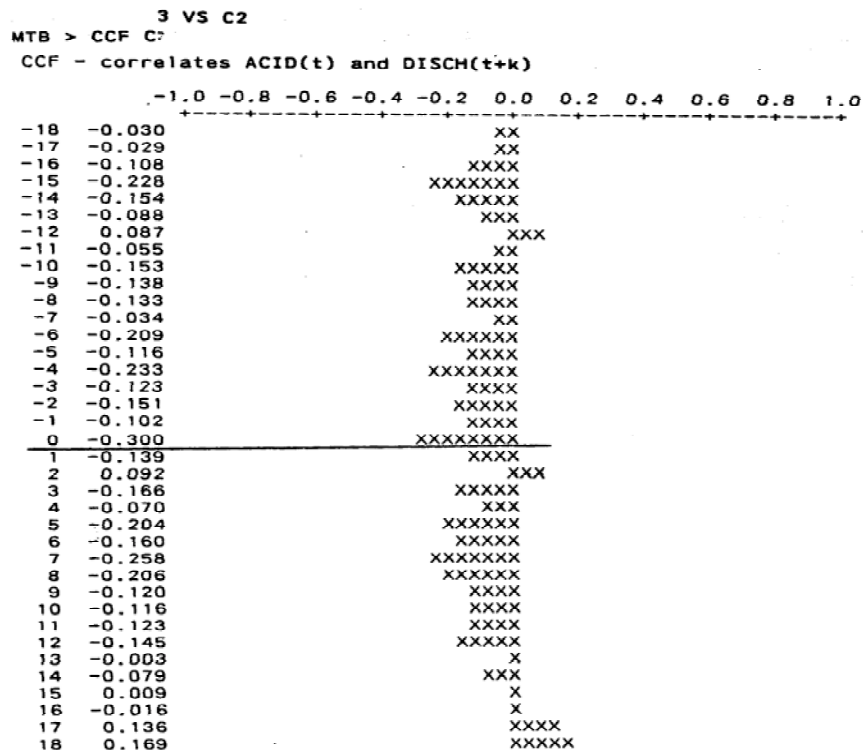
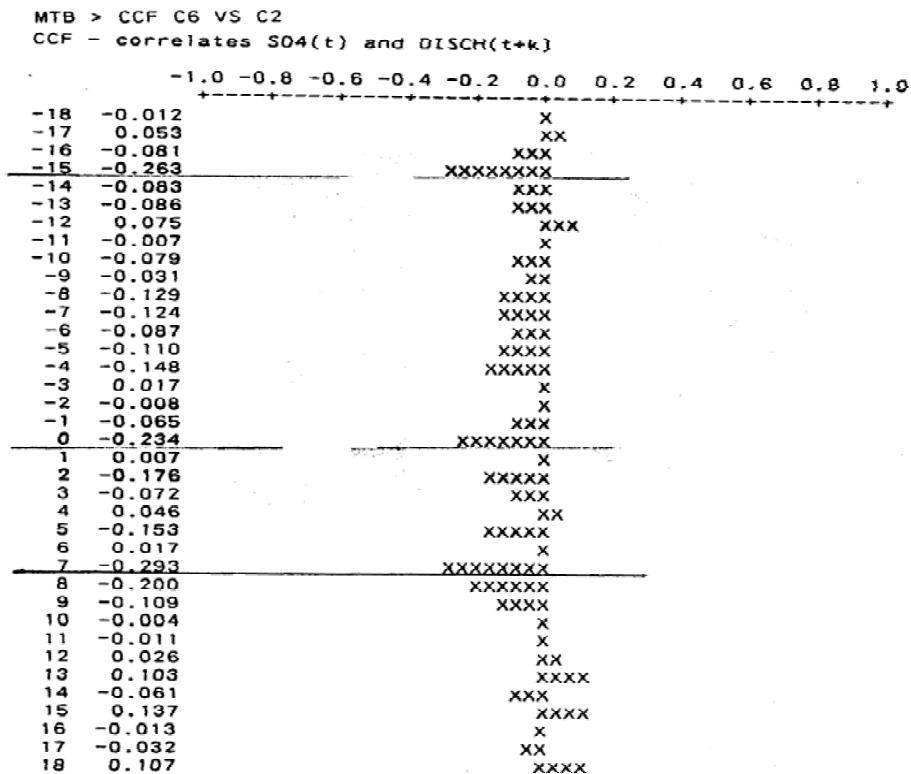


Figure 5.5c: Cross Correlation Function for Sulfate and Discharge



By omitting discharge, it is possible to use the data deck of N=96 and again examine relationships among pairs of variables (see Figure 5.6). The plot of pH against acidity (Figure 5.6a) is curvilinear with pH decreasing rapidly as acidity increases. Below a pH of 3, acidity still increases but the pH stabilizes. Acidity and sulfate (Figure 5.6b) show positive direct linear association with a wide scatter of data points.

Figure 5.6a: Plot of pH vs. Acidity

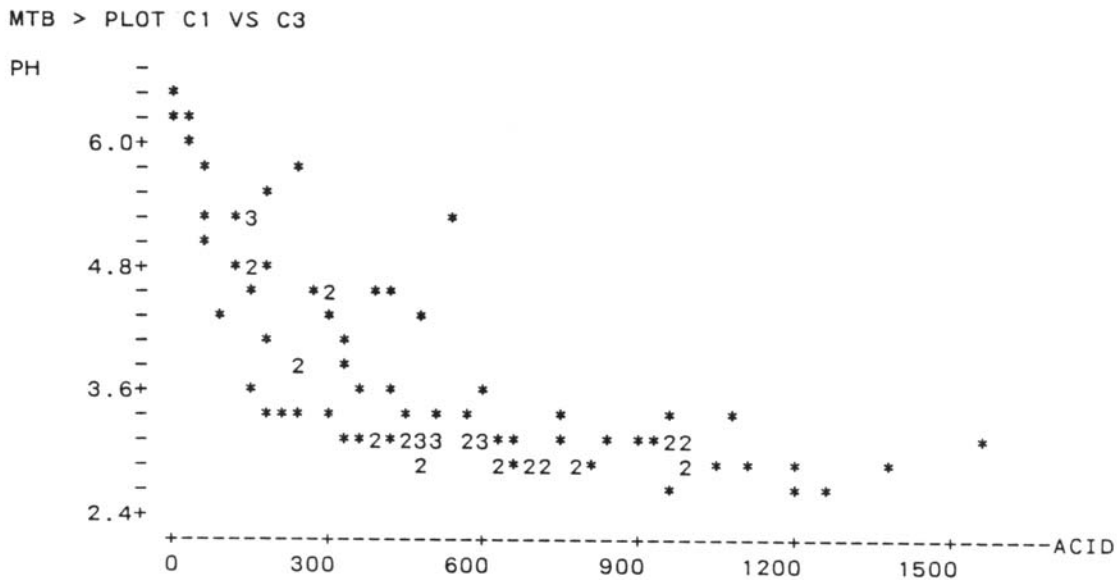


Figure 5.6b: Plot of Acidity vs. Sulfate

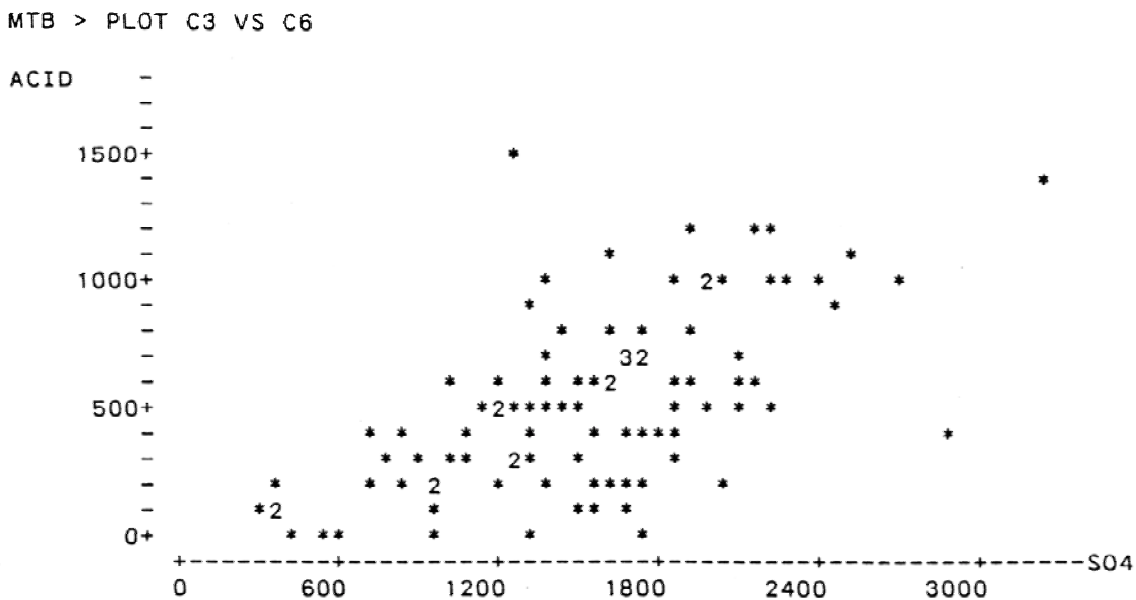
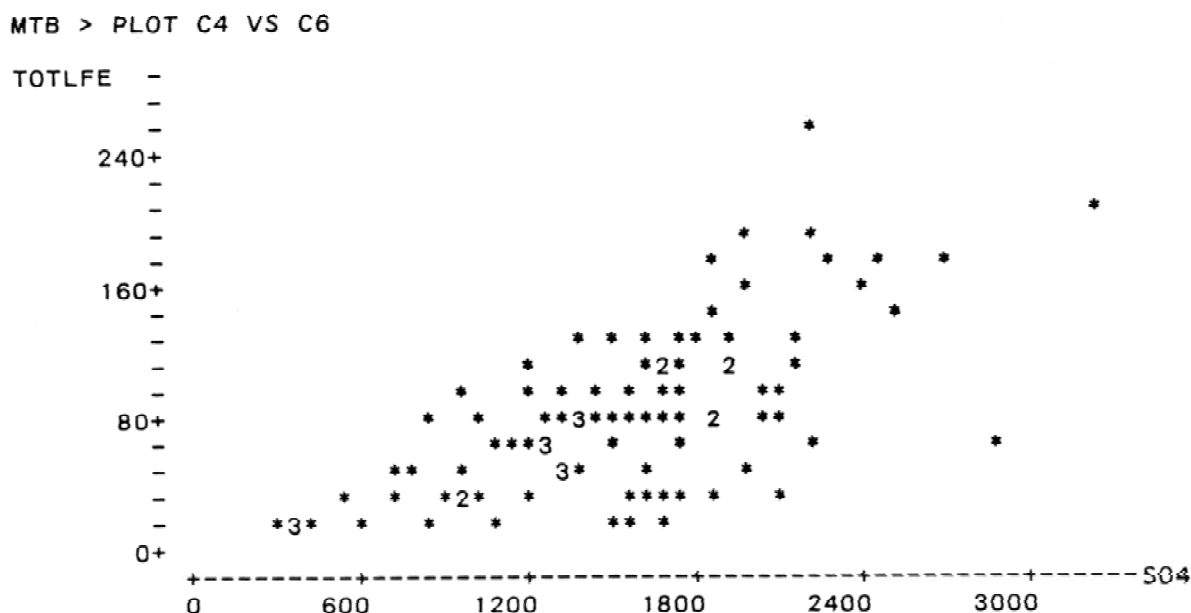


Figure 5.6c: Plot of Iron vs. Sulfate



The importance of these plots is that, despite a wide scatter and tendency to show heteroscedasticity (See Figure 5.6c, total iron vs. sulfate), the association is similar for all pairs of variables (i.e., direct linear association). The comparison of the characteristics of homoscedasticity and heteroscedasticity in bivariate plots of data is described in Chapters 3, 6 and 9 of this report and shown in Figures 6.5a through 6.5c. When the variation of two variables increases as their values increase, heteroscedasticity is present, and it is generally advisable to logarithmically transform these variables, which tends to make the plot of the variables homoscedastic if the standard deviation increases approximately proportionally to concentration prior to transformation.

The persistence of these linear relationships allow us to use one, or at most two, variables for detailed analysis. The conclusions from this analysis may be applied to the other variables. In most cases, there appear to be relationships that are roughly linear. However, the very wide scatter of the data makes the associations rather weak.

Time Series Analysis

Under time series analysis, the data are analyzed in three steps. First, the data may be displayed as graphical plots against time, and quality control limits of two standard deviations (using results from Tables 5.1 and 5.2) may be inserted to show the unusual departures from the mean or median. Second, the data for each variable may be submitted to autocorrelation function analysis (Acf). This permits comparison of variability over time for each parameter and serves to yield a preliminary identification of suitable models for more complex analysis. Third and finally, the data for selected variables are subjected to more complete Box-Jenkins analysis to identify and compare appropriate time series models.

The plot of pH versus time is shown in Figure 5.7a. The most striking feature is the large change in the magnitude of variation after the 50th observation. It appears as if an entirely different environment occurred after the 51st observation (June 30, 1984). Because the two parts of the curve are so different, the two standard deviation limits for the mean underestimate the variation in the later part of the curve. This leads to six values exceeding the two standard deviation limits. It would require data representing a much longer period to determine if this change is a unique circumstance or a regular occurrence.

Figure 5.7b displays a plot of acidity versus time and shows a somewhat different pattern, hence the low degree of association earlier described. Total iron versus time (Figure 5.7c) has a pattern similar to that of acidity versus time, although there is an extreme peak for acidity at time period 73 and iron has smaller peaks at 77 and 79. Sulfate versus time (Figure 5.7d) varies in the same manner as acidity and total iron.

It seems evident that for pH, acidity, total iron, and sulfate there is a break after the 40th observation (Figures 5.7a through 5.7d) reflecting the effect of lime treatment at that time. In this series of graphs, it can be observed that the effect of lime treatment was not persistent, and instead, disappeared with time.

Figure 5.7a: Plot of pH vs. Time

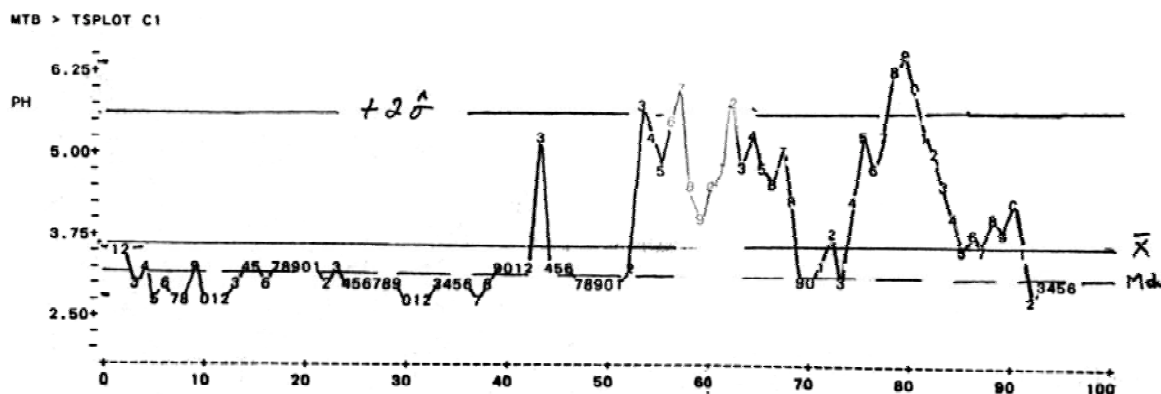


Figure 5.7b: Plot of Acidity vs. Time

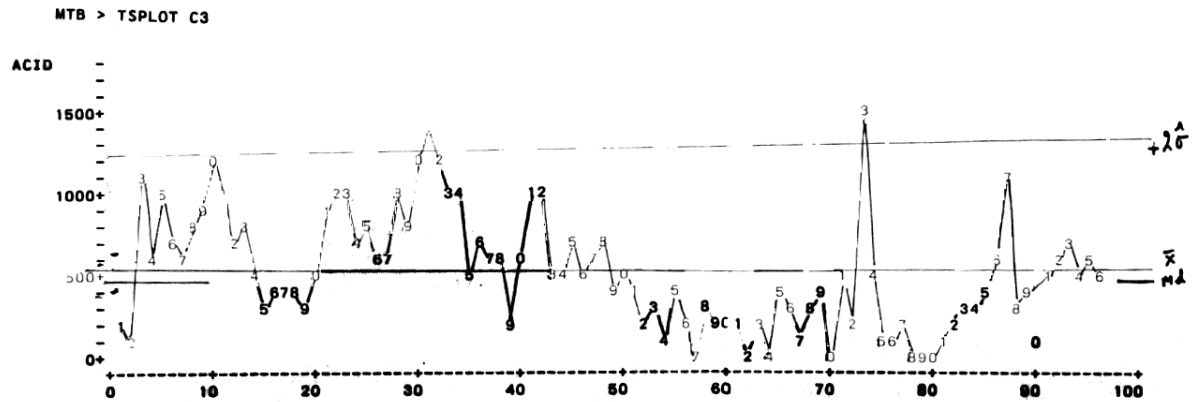


Figure 5.7c: Plot of Iron vs. Time

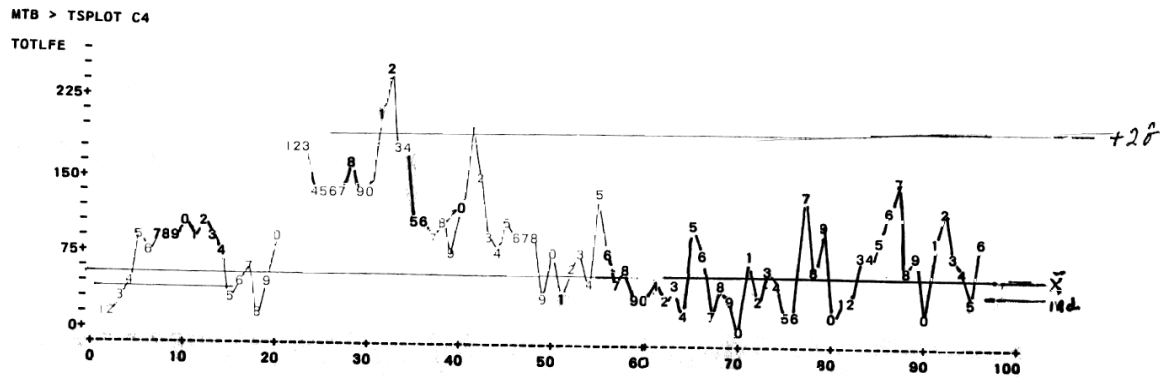
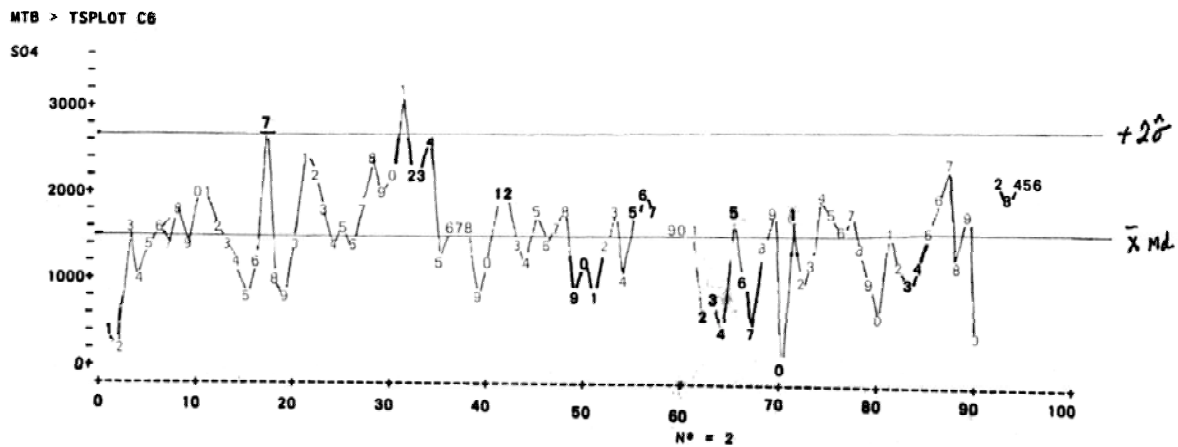


Figure 5.7d: Plot of Sulfate vs. Time



Autocorrelation Functions

It should be noted that the autocorrelation function (Acf) may be used to identify the kind of model which best represents the data for more detailed analysis and curve-fitting. The Acf of pH (Figure 5.8a) shows a sharp decline with increasing lag, and would probably require a first difference to remove this “trend.” Acf’s of acidity (Figure 5.8b) and total iron (Figure 5.8c) are similar and possess similar implications. Sulfate (Figure 5.8d) shows a much weaker degree of autocorrelation but is still of the same general form.

Figure 5.8a: Autocorrelation Function of pH

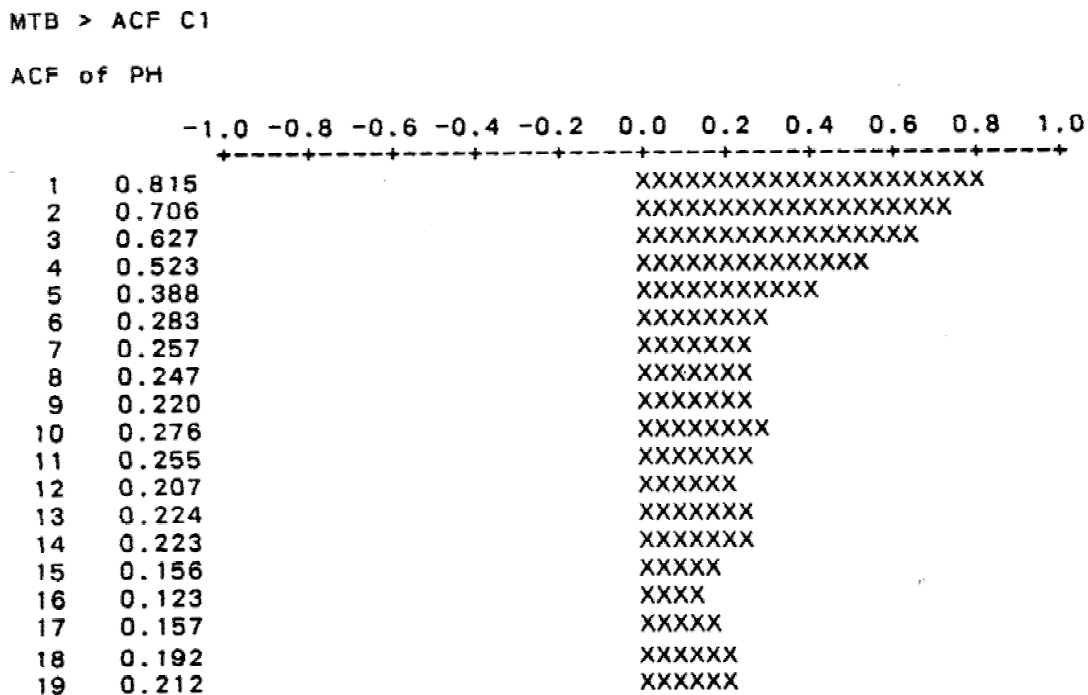


Figure 5.8b: Autocorrelation Function of Acid

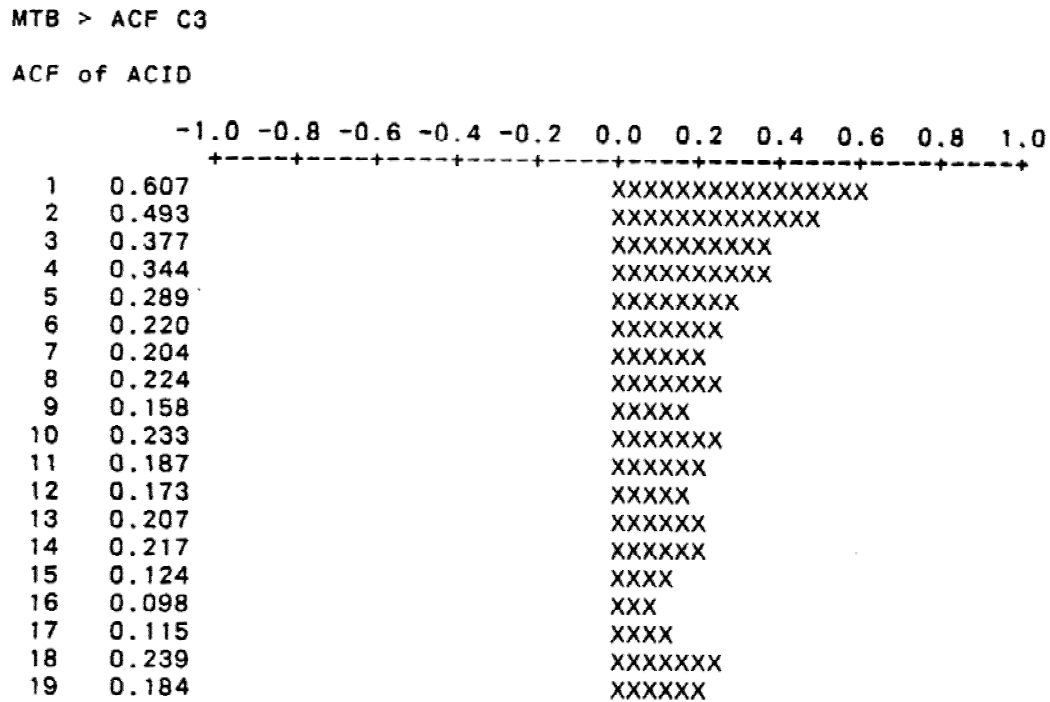


Figure 5.8c: Autocorrelation Function of Total Iron

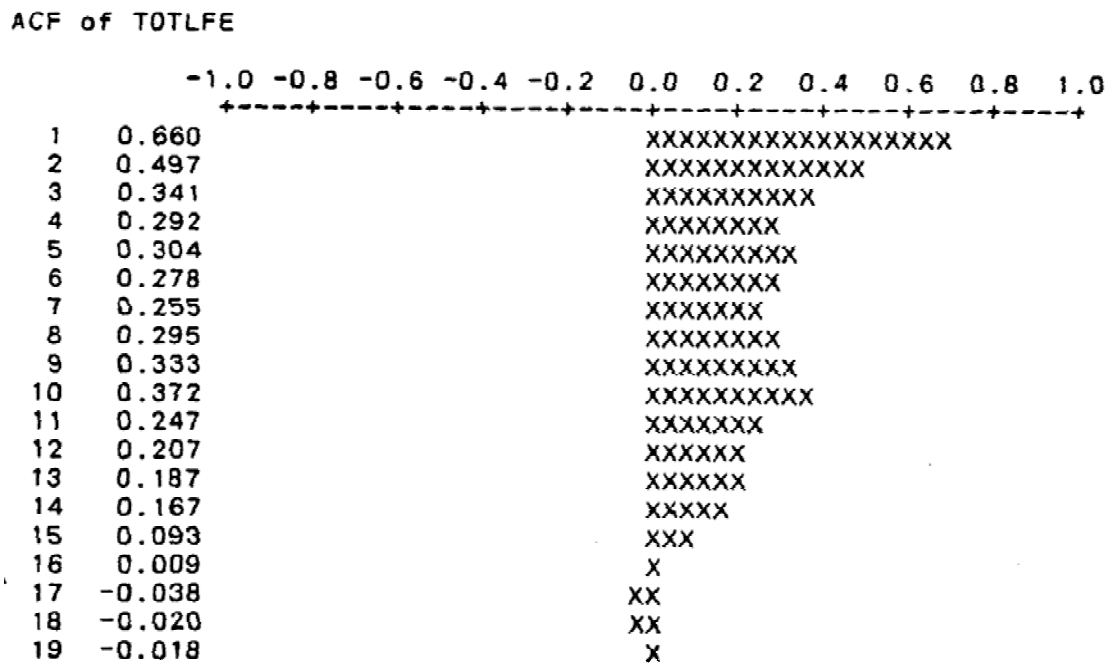
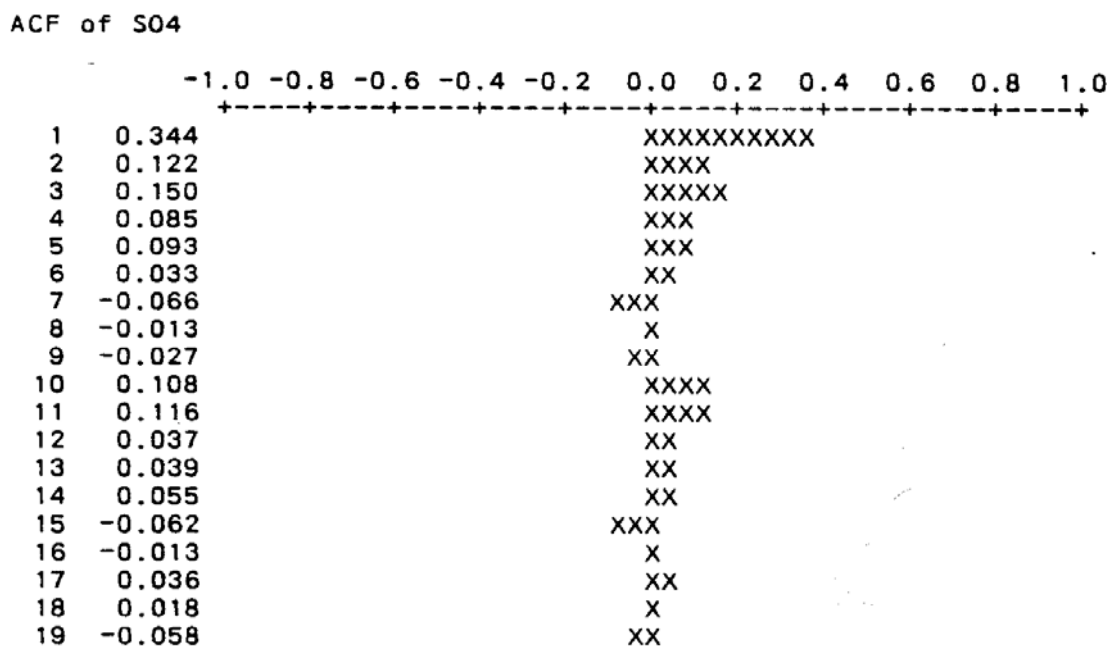


Figure 5.8d: Autocorrelation Function of Sulfate

The ACF of ferrous iron showed no evident pattern and initially, at least, could be considered to show random variation. Ferric iron effectively showed no variation. One cannot but suspect that these variables need careful examination, in regards to field measurement and laboratory testing procedure.

Modeling Selected Variables by Box-Jenkins Time Series Analysis

Three of the variables were chosen for more detailed analysis; pH, sulfate, and ferrous iron. pH shows, essentially, variation that is similar to sulfate. Presumably, they should both possess somewhat similar models. Ferrous iron was included to see if variation was random.

The ACF of first difference for pH gave a chi-square (goodness-of-fit test for the given model) of 40.17 with 25 degrees of freedom yielding a probability of less than 0.05 and greater than 0.02. The original data gave a chi-square of 285.3 with 25 degrees of freedom ($P < 0.001$). Taking a second difference led to an increase in the chi-square value to 70.26 which suggests over-differencing.

The chi-square of 32.56 with 22 degrees of freedom (df) for ACF of residuals after fitting a one step autoregressive AR (1,0,0) model gives a $0.10 > P > 0.05$ (Table 5.3). This effectively reduced the ACF, and the accompanying partial autocorrelation functions (Pacf) possessed what appear to be significant spikes at lags 10 and 19. These spikes were ignored because, to

conclude that they were reflections of real seasonal effects would require the existence of a significant spike at low lags (say at lag 5) and this did not occur. Up to period 42, the residuals are very small. At period 42, there is a serious departure and residuals show larger fluctuations from period 50 onwards.

Table 5.3: Summary of Time Series Models for pH, Clarion Mine

No	Model	Residuals			Standard Deviation	
		Chi-sq.	df	P	Residual	Original
1.	AR(1,0,0)	32.56	22	$0.10 > P > 0.05$	0.572	0.985
2.	MA(0,1,1)	36.26	23	$0.5 > P > 0.2$	0.579	0.985

The standard deviations, after fitting either model, are almost the same (Table 5.3) each representing about a 60% reduction. The relevant equations for the models of the pH variable are:

1. AR: $z_t = 0.821z_{t-1} + 3.676 + a_t$
2. MA: $z_t = a_t - 0.247a_{t-1}$

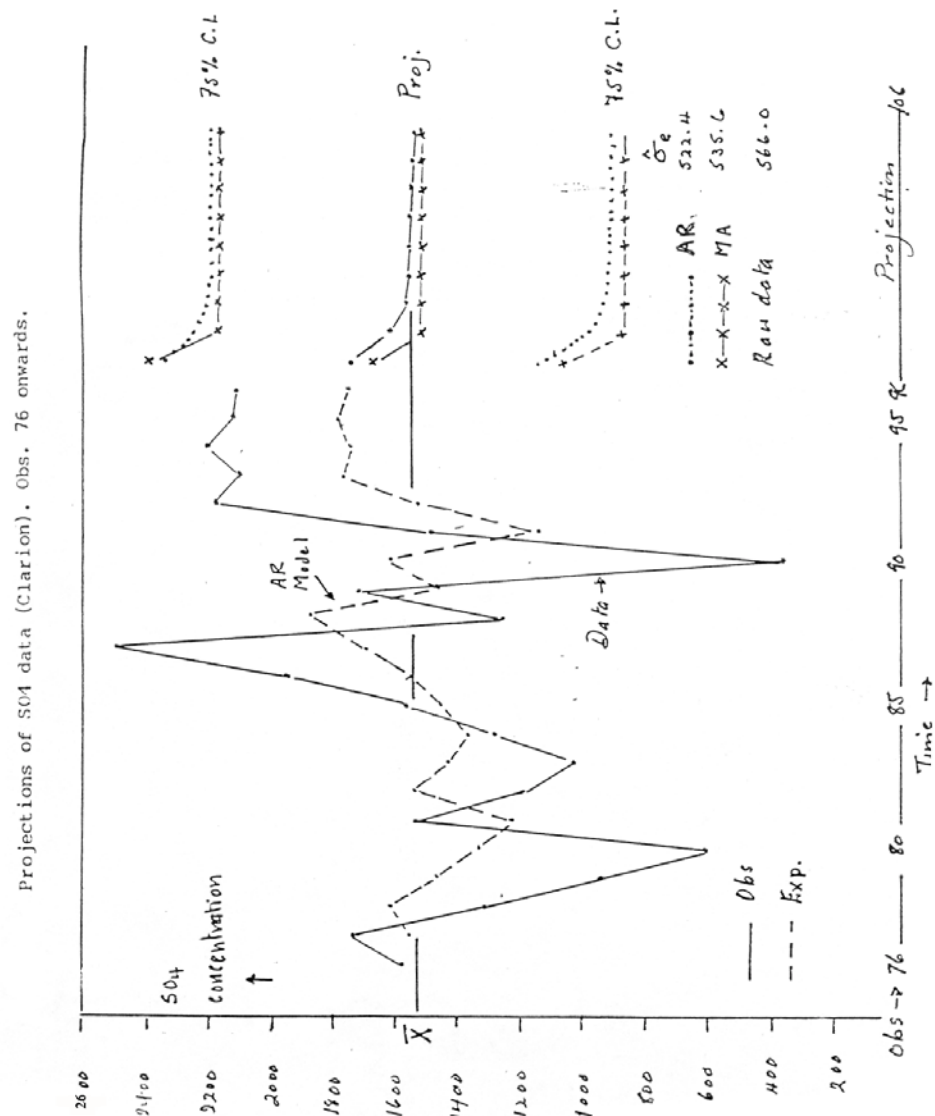
As may be seen in Table 5.4, the two models used for sulfate variation are the AR (1,0,0) and the moving average, MA (0,0,1) models. The chi-square statistics are similar but the AR (1) yields an Acf of residuals without any significant spikes. The MA (1) does not achieve as clean an Acf of residuals.

The standard deviations of the residuals (Table 5.4) from both models offer only minor reduction in the original standard deviation of the raw data (< 10%). A comparison of both models as predictors of future observations is displayed in Figure 5.9. The projections and the 75% confidence limits are similar in both models. It is quite clear that both models show the one step memory and then approximate the overall mean value for the next nine periods. It is fairly evident in Figure 5.9, that the expected values from the AR (1) model fluctuate around the overall mean and fail to duplicate closely, the wide swings present in the raw data. This is because the model is based on the entire record of 96 observations and the fluctuations are very large during the first 35 and the last 30 periods (see Figure 5.7d).

Table 5.4: Summary Statistics for Time Series Models of SO₄ from Clarion Site

N	Model	Residuals			Standard Deviation	
		Chi-sq.	df	P	Residual	Original
1.	AR(1,0,0)	9.184	22	> 0.99	522.3	566.0
2.	MA(0,0,1)	9.204	22	> 0.99	535.6	566.0

Figure 5.9: Projections of Sulfate Data



The relevant equations for the models of the sulfate variable are:

1. AR (1): $z_t = 0.348z_{t-1} + 1550.9 + a_t$
2. MA (1): $z_t = a_t + 0.345a_{t-1} + 1526.1$

Four models were used in an attempt to find a “best” fit for the ferrous iron variable. The usual one step models AR (1) and MA (1) led to satisfactory results which were very similar (Table 5.5). The autocorrelation functions of the residuals from both led to chi-squares of 20.50 and 26.10 respectively. The degrees of freedom were 23 in both cases, and the probability statements are similar. Hence, in effect, either of these models are adequate representations of the raw data. The standard deviations of the residuals were close (29.81 and 31.00 respectively). However, these standard deviations represent very little improvement over the standard deviation of the raw data (see Table 5.5).

Since there were some irregular spikes in the lag 2 position of the autocorrelation functions of the residuals from the first two models, more complex models were applied, (MA (2) and an ARMA(1,1)). From Table 5.5, it can be seen that the outcomes, in terms of probability of achieving a chi-square value as large as these from a white noise (i.e., random) series, is very likely. The standard deviations are close to those of the simpler models and nothing was gained by attempting to fit these more elaborate models.

Table 5.5: Summary of Time Series Models for Ferrous Iron, Clarion Site

No.	Model	Residuals			Standard deviation	
		Chi-sq.	df	P	Residual	Original
1.	AR(1,0,0)	20.50	23	$0.6 < P < 0.7$	29.81	34.46
2.	MA(0,0,1)	25.10	23	$0.3 < P < 0.4$	31.00	34.46
3.	MA(0,0,2)	17.60	22	$0.7 < P < 0.8$	29.76	34.46
4.	ARMA(1,0,1)	20.60	22	$0.5 < P < 0.6$	29.96	34.46

The relevant equations for the models of the ferrous iron parameter are:

1. AR (1): $z_t = 0.512z_{t-1} + 48.2 + a_t$
2. MA (1): $z_t = a_t + 0.411a_{t-1} + 48.4$
3. MA (2): $z_t = 48.34 + a_t + 0.466a_{t-1} + 0.302a_{t-2}$
4. ARMA (1,1): $z_t = 48.18 + 0.545z_{t-1} + a_t - 0.044a_{t-1}$

Significance tests of the coefficients for ferrous iron suggest they are likely to be real except for the coefficient of the moving average (MA) term in the ARMA model. Because the confidence limits include zero, this model is rejected.

Quality Control Limits

There is a very large number of methods for defining quality control limits and there are arguments for and against all of them. This section of the chapter is an attempt to compare different limits for the Clarion site data. Unfortunately, the standard deviations and spreads for the variables in this data set are very large, and may be atypical. Also, the probability statements refer to comparisons of single samples; multiple comparisons using several samples may require inflation of the control limits or a reduction in the probability statements.

Table 5.6 contains the statistics from which the quality control limits may be derived. The original summary statistics for this data set ($N=79$) are shown in Table 5.2, and Appendix C contains a table of various spreads for this data set. The column in Table 5.6 labeled H-spr/1.349 is included because it is supposed to be an approximate estimate of the standard deviation (Velleman and Hoaglin, 1981, p.54). These values may be compared with the corresponding standard deviations in the adjacent column. The H-spread estimate for the standard deviation of pH is smaller than the observed value. The estimate for the standard deviation of discharge is much smaller than (one-third of) the observed value, probably reflecting the marked skewness of these data, which arises from a few extremely large values. The H-spread estimate for acidity is larger than the observed value, and is suspected to be a reflection of the skewed data. The estimates for sulfate, total iron, ferrous iron and ferric iron are all similar to their observed values.

Table 5.6: Comparison of Statistics used to calculate the QC limits ($N' = 79$)

Variable	Mean	Median	H-spread	C-spread	Standard Deviation	H-spread/1.349
pH	3.624	3.16	1.06	3.38	0.967	0.786
Discharge	12.57	6.7	8.745	50.44	22.37	6.48
Acid	556.1	499	562.5	1381	361.2	416.98
Total Iron	86.7	78.5	73	181.5	53.45	54.11
Ferrous Iron	51.23	40	47.45	128.2	35.92	35.17
SO ₄	1586.3	1619	716	2125.99	558.6	530.76
Ferric Iron	35.47	26	49.15	99.1	33.8	36.43

A number of possible spreads which could be used to set up quality control limits are listed in Table 5.7. The first example is the conventional spread of the mean plus and minus twice the standard deviation. In a normal frequency distribution this would include about 95 percent of the distribution or, alternately, it is expected that about 5 observations in every 100 would fall outside these limits. The constraint of strict normality may be relaxed considerably so that this is a reasonably general confidence interval. This spread would be used to compare to individual results (i.e., $N' = 1$).

Table 5.7: Comparison of QC Limits (Spreads) around Mean and Median

	Mean \pm 2 Standard Deviation		Mean \pm 2 Standard Deviation / $\sqrt{N'}$		Median \pm 1.58 * H-spread / $\sqrt{N'}$	
	$N' = 79$					
	Variable	LL	UL	LL	UL	LL
pH	1.69	5.56	3.41	3.84	2.97	3.35
Discharge	-32.2	57.3	7.5	17.6	5.1	8.3
Acid	-166.3	1278.5	474.8	637.4	399.0	599.0
Total Iron	-20.2	193.6	74.7	98.7	65.5	91.5
Ferrous Iron	-20.61	123.07	43.15	59.31	31.57	48.43
SO ₄	469.1	2703.5	1460.6	1712.0	1491.7	1746.3
Ferric Iron	-32.1	103.1	27.9	43.1	17.3	34.7

	Median \pm 1.58 * H-spread / $\sqrt{N'}$		Mean \pm 2 Standard Deviation / $\sqrt{N'}$	
	$N' = 18$			
	Variable	LL	UL	LL
pH	2.77	3.55	3.17	4.08
Discharge	3.4	10.0	2.0	23.1
Acid	289.5	708.5	385.8	726.4
Total Iron	51.3	105.7	61.5	111.9
Ferrous Iron	22.33	57.67	34.30	68.16
SO ₄	1352.4	1885.6	1323.0	1849.6
Ferric Iron	7.7	44.3	19.5	51.4

If the number of samples is taken into account it must be emphasized that the calculated interval refers to means of sets of samples of size N' ; for example, if the number of observations is chosen as base, then $1/\sqrt{N'}$, in this case, $= 1/\sqrt{79} = 0.113$, or for $2\hat{\sigma}(1/\sqrt{N'}) = 0.226\hat{\sigma}$. These limits are much too restricted. Relaxing this requirement, to say an $N' = 18$, gives $0.471\hat{\sigma}$, and this again refers to means based on sample sizes of 18. This would appear to be too restrictive, because too many observations would fall beyond these limits. Similar features apply to each estimate containing N where $\sqrt{N'} > 1$.

Since the sample size is usually one ($\sqrt{N'} = 1$), the multiplier will be 2 times $\hat{\sigma}$ or some equivalent in non-parametric form. The intervals (quality control limits) listed in Table 5.7 show a comparison of the conventional parametric limits (based upon $2\hat{\sigma}$), together with non-parametric limits ($1.58(\text{H-spread})/\sqrt{N'}$) where the sample sizes are $N' = 79$ and $N' = 18$.

Three different estimates of quality control limits around the median are given in Table 5.8: the median plus or minus the [C-spread], the median plus or minus 1.58 times the [C-spread] over root N , and the median plus or minus 3 times the H-spread. The conventional limits (means 2

$\hat{\sigma}$) are given for comparison in the last column. The spreads are obtained from the Table in Appendix C.

Table 5.8: Comparison of QC Limits around the Median using Various Forms of Spread

	Median \pm C-spread		Median $\pm 1.58^*$ C-spread $/\sqrt{N'}$		Median $\pm 3^*$ H-spread		Mean $\pm 2^*$ Standard Deviation	
Variable	LL	UL	LL	UL	LL	UL	LL	UL
pH	-0.22	6.54	1.38	4.94	-0.02	6.34	1.69	5.56
Discharge	-43.7	57.1	-19.9	33.3	-19.5	32.9	-32.2	57.3
Acid	-882.0	1880.0	-228.3	1226.3	-1188.5	2186.5	-166.3	1278.5
Total Iron	-103.0	260.0	-17.1	174.1	-140.5	297.5	-20.2	193.6
Ferrous Iron	-88.20	168.20	-27.52	107.52	-102.35	182.35	-20.61	123.07
SO ₄	-507.0	3745.0	499.3	2738.7	-529.0	3767.0	469.1	2703.5
Ferric Iron	-73.1	125.1	-26.2	78.2	-121.5	173.5	-32.1	103.1

The median \pm C-spread compares reasonably well with the median $\pm 3^*$ (H-spread) in Table 5.8 except for discharge where the latter is much smaller than the former. The quality control limits around the mean yield smaller spreads than either the 3^* (H-spread) or the C-spread, except for discharge. The value of the mean $+ 2\hat{\sigma}$ compares well with the median $+ \text{C-spread}$ for discharge.

These comparisons of quality control limits shown in Tables 5.7 and 5.8 are more easily understood if the description is illustrated in graphs. Figure 5.7a is a graph of the pH of the discharge from the Clarion site with the mean and median inserted. It is obvious that the extremely high values after the 50th observation (i.e., after treatment begins), affect the mean much more strongly than the median. The difference between the mean and the median is largely due to the pronounced skewness induced by these few large values.

The C-spread and the 3^* (H-spread) quality control limits in Table 5.8 compare very closely. If these limits are used, only one value falls on or near them. About 7 values fall beyond the 2 sigma limits in Figure 5.7a. The spread of 1.58^* (H-spread $/\sqrt{N'}$) is more constraining than these 2 sigma limits; if it were plotted on Figure 5.7a, 14 observations would fall on or beyond this value of spread.

If adjustment is made for a sample size of $N' = 6$, the limits are much more restrictive and the majority of values after the treatment was initiated fall beyond this limit. The lower quality control limits for pH in Table 5.8 fall outside the limits of this graph, but are of little interest in the present circumstances. For pH, these arguments are mostly illustrative because prior to treatment, the values vary around the median of 3.16, indicating the acidic nature of the discharge. After treatment (after the 50th observation in Figure 5.7a), the pH frequently exceeds 5, but only one value exceeds 6. From the 85th observation onwards, the pH has returned to on or below the median value.

The second graphical example of quality control is the plot of sulfate as shown in Figure 5.7d. In both Figures 5.7a and 5.7d it is assumed that the observations are evenly spaced in time, which is not always true (see Figure 4.2 in Chapter 4). In Figure 5.7d, the mean and median coincide fairly closely, suggesting a symmetrical frequency distribution. It seems obvious that the spread of median $\pm 3 * (H\text{-spread})$ is much too wide (i.e., 3717.0); if it were plotted on Figure 5.7d, no observation would come close to it. The spreads of mean plus or minus two sigma and the median $\pm 1.58 * (H\text{-spread} / \sqrt{N'})$ are very similar and either would be equally effective, although the $2 \hat{\sigma}$ limits plotted on Figure 5.7d appear to be more sensitive.

In conclusion, no simple recommendation on quality control limits can be made on the basis of these observations of the Clarion site, which may or may not be representative. It seems likely that establishment of the form of the frequency distribution, particularly symmetry, appears to be most desirable when setting up the quality control limits. It seems clear in this analysis that the limits are not consistent from variable to variable. If this is true in the analyses of data from different sites, then perhaps different forms of spread with different limits may be necessary for each variable.

Summary

It seems clear from the data that there was a marked change in the environment after the 50th observation (May 8, 1984). This is confirmed by the knowledge that “Limestone application was performed in May and June 1984” (Lusardi and Erickson, 1985, p. 318). These authors also conclude that “one year after the limestone application, the water quality in the seeps reflected no substantial inhibition or neutralization. Improvements in water quality noted in late 1984 have not persisted.” pH shows marked improvement (less acidic water) from June 30, 1984 onwards. However, by April 5, 1986 the pH has returned to pre-treatment levels; these changes are in accord with the conclusions given above. Nevertheless, discharge also shows a change and fluctuates over a much larger range after the treatment date. It is doubtful whether this can be attributed to the treatment.

The time series plot for acidity (Figure 5.7b) fluctuates above the mean up to the 50th observation and then becomes much less variable until just beyond the 70th observation. There is a large spike of increased acidity at 75 and then acidity declines back to the mean value from the 90th observation onwards.

In the case of total iron, the first 19 observations vary closely around the mean of the entire series; then, from observation 20 to 45, total iron shows much larger fluctuations, way above the mean. From the 45th to 55th observation, the variations in concentration are suppressed and from 55th observation onwards, the variability increases but remains around the mean value. Sulfate varies roughly in parallel with acidity and no special effect can be attributed to treatment.

